[CANCER RESEARCH 61, 4916–4922, June 15, 2001]

# A Novel N-*ras* Mutation in Malignant Melanoma Is Associated with Excellent Prognosis[1]

**Anouk Demunter,[2] Mohammad Reza Ahmadian, Louis Libbrecht, Marguerite Stas, Mathijs Baens, Klaus Scheffzek, Hugo Degreef, Chris De Wolf-Peeters, and Joost J. van den Oord**

*Laboratory of Morphology and Molecular Pathology, Departments of Pathology [A. D., L. L., C. D. W-P., J. J. v. d. O.], Surgical Oncology [M. S.], and Dermatology [H. D.], Katholieke Universiteit Leuven, Leuven 3000, Belgium; Human Genome Laboratory, Center for Human Genetics, Flanders Interuniversity Institute for Biotechnology, Leuven 3000, Belgium [M. B.]; Max-Planck Institute, Dortmund 44227, Germany [M. R. A.]; and European Molecular Biology Laboratory, Heidelberg 69120, Germany [K. S.]*

## ABSTRACT

**Mutations in the *ras* gene are key events in the process of carcinogenesis; in particular, point mutations in codon 61 of exon 2 of the N-*ras* gene occur frequently in malignant melanoma (MM). We searched for point mutations in the N-*ras* gene in a large series of primary and metastatic MM from 81 different retrospectively selected patients using the very sensitive denaturing gradient gel electrophoresis technique, followed by sequencing. The classical codon 12 and codon 61 mutations were found in 21 and 17% of the cases, respectively. No codon 13 mutation was found. A novel mutation at codon 18 of exon 1, consisting of a substitution of alanine (GCA) by threonine (ACA), was found in 15% of the primary MMs but in none of the metastatic MMs. All of the other cases were free of mutations. Using microdissected cells from distinctive MM growth phases as source of DNA for mutation analysis, this particular N-*ras* exon 1 mutation at codon 18 was already present in the radial growth phase and preserved throughout the successive growth phases; it was also found in a dysplastic nevi in continuity with a MM, indicating a clonal relationship between both lesions. Our findings also illustrate the clonal relationship between the distinctive growth phases in MM and suggest the codon 18 mutation to occur early in MM development. The MM in patients with this mutation were significantly thinner than those without a codon 18 mutation ($P = 0.0257$). Statistical analysis, comparing the group of codon 18 patients with the group of patients with the classical mutations and without mutations, revealed a highly significant difference in overall outcome. The cumulative probability of developing metastasis was significantly lower for the group patients with a codon 18 mutation ($P = 0.0130$). We can thus conclude that this codon 18 mutation identifies a group of patients with better prognosis than patients with melanoma that harbor wild-type sequence or classical activating point mutations in codon 12 or 61.**

**Preliminary nucleotide binding measurements could not detect a difference between wild-type Ras protein and the mutant Ras(A18T) protein. However, for a precise elucidation of the role of the N-Ras(A18T) mutant in melanoma, additional studies aimed to measure the affinity to guanine nucleotide exchange factors and GTPase-activating proteins are needed.**

## INTRODUCTION

Most malignant tumors are characterized by the occurrence of multiple mutations throughout the genome, which will alter the products of a number of genes, controlling cell growth and differentiation. These mutations will accumulate in a step-wise manner during tumor progression. Mutations in many different genes have been described in MM[3] including the *ras* genes. This family consists of three functional oncogenes, H-*ras*, K-*ras*, and N-*ras*, which encode highly similar proteins with molecular weights of $M_r$ 21,000 (1). Normal p21 Ras proteins, showing structural and functional resemblance with the G-proteins (controlling adenylate cyclase) are involved in the transduction of external stimuli, induced by the binding of growth factors or factors involved in cell differentiation to a specific receptor such as receptor tyrosine kinase. Activated Ras proteins have been shown to interact with numerous downstream targets, to activate several different signaling pathways, and subsequently become inactivated (2, 3). Mutated Ras proteins, however, have lost the ability to become inactivated and thus stimulate cellular growth and differentiation continuously (3). Experimental evidence indicates that inhibition of their GTPase activity is the preferred mechanism of activation of oncogenic Ras proteins (4–6).

Mutations in naturally occurring *ras* oncogenes have been found in codons 11, 12, 13, 59, and 61 (7–11). In MM, mutations in *ras* oncogenes have repeatedly been detected, although their role in the pathogenesis of MM still remains poorly understood. Using cultured melanoma cells, Albino *et al.* (12) found mutations in 24% of the cases, in contrast to 5–6% of the noncultured primary and metastatic MMs. Using mutation-specific oligonucleotide hybridization, van't Veer *et al.* (13) detected N-*ras* mutations in 7 of 37 (19%) melanoma tumor samples from sun-exposed body sites, and Ball *et al.* (14) investigated 100 paraffin-embedded primary and metastatic MMs using dot blot hybridization and found a mutation frequency of 36%. In all of these studies, the overwhelming majority of mutations were located in codon 61 of N-*ras* exon 2, attributable to the preferential formation of cyclobutane dimers at this site after UV irradiation (15).

Thus far, the activating *ras* mutations have not been localized to distinctive growth phases of MM, and hence, it is as yet unknown whether they are involved in early or late stages of tumor progression. We have studied the occurrence of N-*ras* mutations in the distinctive tumor progression stages of MM using microdissected cells, isolated from distinctive growth phases, as a source of DNA for mutation analysis. During this study, we have found a novel mutation in codon 18 of N-*ras* exon 1, which will be the subject of this report. To determine the clinical and biological significance of this mutation, we evaluated clinical and histological data of the patients and introduced this mutation into H-*ras* to reveal the biochemical properties of the mutant protein.

## MATERIALS AND METHODS

**Cell Lines.** N-*ras* transfectants 11A15 and 7D8 and melanoma cell line Mel-634 were kindly provided by C. Aarnoudse (Department of Clinical Oncology, University Hospital, Leiden, the Netherlands; Ref. 16). The MOLT-4 cell line was provided by J. Van Pelt (Laboratory of Hepatology, University Hospitals Leuven, Leuven, Belgium; Ref. 17).

**Patient Material.** Sixty-nine primary MMs and 33 melanoma metastases from 81 different patients were used for this study. These cases were randomly

Received 1/10/01; accepted 4/11/01.

The costs of publication of this article were defrayed in part by the payment of page charges. This article must therefore be hereby marked *advertisement* in accordance with 18 U.S.C. Section 1734 solely to indicate this fact.

[1] Supported in part by Grant OT/98/33 from the Katholieke Universiteit Leuven (to A. D.).

[2] To whom requests for reprints should be addressed, at Department of Pathology, Laboratory of Morphology and Molecular Pathology, University Hospital St. Rafael, Minderbroederstraat 12, 3000 Leuven, Belgium. Phone: 32-16-33-66-44; Fax: 32-16-33-65-48; E-mail: anouk.demunter@uz.kuleuven.ac.be.

[3] The abbreviations used are: MM, malignant melanoma; RGP, radial growth phase; VGP, vertical growth phase; DGGE, denaturing gradient gel electrophoresis; DOP-PCR, degenerated oligonucleotide-primed PCR; ncn, nevocellular nevus; GppNHp, guanosine β,γ-imidotriphosphate; mGppNHp, mutant GppNHp; SSCP, single-strand conformation polymorphism; GAP, GTPase-activating protein; GEF, guanine nucleotide exchange factor; TIL, tumor-infiltrating lymphocyte.

retrieved from the archives of the Department of Pathology starting from 1985 until 2000. From 19 patients, both the primary MMs and the metastases were available for analysis. Seven MMs were associated with ncn including 1 dermal ncn, 4 compound ncn, 1 lentigo simplex, 2 dysplastic ncn, and 1 congenital nevus. From 62 cases, the material was received fresh; a representative part of the material was snap frozen in liquid nitrogen-cooled isopentane and stored at −80°C until used. The other part was fixed in neutral buffered formalin, embedded in paraffin, and used for routine histology. To evaluate fixation-related artifacts, both frozen and paraffin-embedded material from 10 patients were analyzed. Of the other cases, either frozen or paraffin-embedded tissue was available for study. Metastatic MMs were analyzed by DNA extractions from whole tissue sections if >80% of the surface was involved by neoplastic tissue; in primary MMs and associated ncn, clusters of neoplastic cells were microdissected and used as source of DNA (see below).

**Follow-Up of Patients.** All cases had been treated surgically according to standard procedure, and the resection margins were negative in all cases of primary MM. Of the 69 randomly selected patients with a primary MM, 51 had been followed for at least 6 months after resection of the tumor and clinical examinations, X-ray, sonography, and analysis of serum liver enzyme levels revealed no metastasis at the time of diagnosis. These 51 cases, all stages I and II [according to the American Joint Committee on Cancer system (18)], were then used for statistical analysis in a retrospective study. The date of the histopathological diagnosis was used as the entry date. The duration of follow-up was the time (measured in months) from the diagnosis to either the detection of metastasis, the date of death attributable to a cause unrelated to the MM, or the date of the most recent control. All patients underwent regular follow-up according to a standard protocol that included clinical examinations, X-ray and sonography, and analysis of serum liver enzyme levels.

All primary MMs were reevaluated histologically, and in each case, the classical histological prognostic criteria were assessed according to standard criteria (19). The following baseline characteristics were used in the statistical analysis: sex, age, thickness according to Breslow (≤1 mm; 1.01–2.0 mm; 2.01–4.0 mm; or >4 mm), mitotic index (≤6/mm$^2$ or >6/mm$^2$), tumor infiltration by lymphocytes (TILs), ulceration, regression, vascular invasion, and mutations in codons 12, 18, and 61 of the N-*ras* gene. Histopathological reevaluation of all cases occurred without knowledge of the mutation status of N-*ras* codons 12, 18, and 61 and according to standard criteria.

**Microdissection.** Buffered formalin-fixed, paraffin-embedded, and/or frozen sections of all primary MMs, showing well-recognizable, distinctive tumor progression phases on histology, were subjected to microdissection. After staining with H&E, both frozen and paraffin-embedded tissue sections were digested by incubation at 40°C for 3 h in collagenase H (Boehringer Mannheim, Brussels, Belgium). Subsequently, the various tumor progression phases of the MMs were identified, *i.e.*, the "pure" RGP, restricted to the epidermis; the "invasive" RGP, characterized by small nonexpansile clusters or single neoplastic cells in the papillary dermis; the VGP, consisting of expansile cohesive nodules of neoplastic cells in the dermis, and/or the metastatic phase. Depending on the tumor-progression phase, 20–100 cells were collected per growth phase from consecutive sections. The cells were aspirated with another sterile glass needle, transferred to an Eppendorf tube, and resuspended in 5 μl of a solution (260 mM Tris-HCl, pH 9.5; 65 mM $MgCl_2$) containing 7 mg/ml proteinase K (Boehringer Mannheim). Samples were incubated overnight at 55°C, followed by boiling for 1 min to inactivate proteinase K. All material was used for DOP-PCR. To exclude constitutional base changes, nonmelanoma tissue from three patients was also studied.

**DOP-PCR.** DOP-PCR was performed on a thermocycler (Perkin-Elmer 480; Perkin-Elmer Applied Biosystems, Lennik, Belgium) in two separate phases. Four initial cycles (preamplification step) were carried out in a 10-μl reaction mixture [using ThermoSequenase (Amersham Pharmacia, Roosendaal, the Netherlands) and a high salt buffer] at low stringency conditions, which was followed by 30 cycles in a 40-μl reaction volume [using AmpliTaq polymerase LD (Perkin-Elmer Applied Biosystems) and a low salt buffer] at high stringency conditions. Both PCR reactions contained the UN1 primer (5′-CCG ACT CGA GNN NNN NAT GTG G-3′, with *n* = A, C, G, or T), allowing universal amplification of genomic DNA (20). Reagents, volumes, and reaction are described previously by Kuukasjärvi *et al.* (21). The product was purified (Qiagen Westburg, Leusden, the Netherlands) before further use.

**Specific PCR.** Exons 1and 2 of the N-*ras* gene were selectively amplified using PCR. Thermal cycling was carried out with the GeneAmp PCR system 9600 (Perkin-Elmer Applied Biosystems) in final volumes of 50 μl, containing 10 mM Tris-HCl (pH 8.3), 50 mM KCl, 2 mM $MgCl_2$, 200 μM each deoxynucleotide triphosphate, 0.2 μM of each primer [for N-*ras* exon 1: forward, 5′-CTGGTGTGAAATGACTGAGT-3′ and reverse, 5′-[GC]-GGTGGGATCATATTCATCTA-3′; for N-*ras* exon 2: forward, 5′-GTTATAGATGGTGAAACCTG and reverse, 5′-ATACACAGAGGAAGCCTTCG (22)], 500 ng of DNA and 2.5 units of Taq polymerase (AmpliTaq Gold; Perkin-Elmer). A 40-bp GC-clamp was attached to the reverse primer ([GC] = CGCCCGCCGCGCCCCGCGCCCGGCCCGCCGCCCCCGCCCG) and proved to be sufficient for the demonstration of the cell line mutations in both exons of N-*ras*. The amplification protocol consisted of 40 cycles with denaturation at 94°C, annealing at 50°C, and extension at 72°C for 1 min. An initial denaturation step of 94°C for 10 min and a final incubation at 72°C for 2 min were included.

**DGGE.** To test the DGGE conditions needed for this approach, cell lines harboring well-known mutations were analyzed, *i.e.*, MOLT4 (heterozygous for mutation in N-*ras* codon 12 position 1), N-*ras* transfectants 11A15 [518-L1 (61-Leu/L)] and 7D8 [MD3A-K (61-Lys/K)], and the melanoma cell line Mel-634 (with a natural arginine mutation in codon 61 of N-*ras*). A 12% polyacrylamide gel containing a gradient of urea and formamide from 20 to 50% was sufficient to detect all of the cell line mutations. To demonstrate the sensitivity of the DGGE assay, the mutant PCR product was mixed with the corresponding wild-type PCR product to generate heteroduplexes, *i.e.*, hybrids formed between mutant and wild-type DNA strands (Fig. 1*A*). DNA from MOLT-4 cell line (heterozygous for mutation in N-*ras* codon 12 position 1) was serially diluted with normal human spleen and revealed a detection sensitivity of 2.5% mutant DNA in wild-type sample (Fig. 1*B*).

Forty μl of PCR product was dried out and loaded on the gels to run at 170 V for 4 h in 1× TAE buffer (40 mM Tris, 20 mM acetic acid, and 1 mM EDTA, pH 8.3) kept at a constant temperature of 60°C. DNA sequencing was done to confirm the results on the DGGE gel.

**Biochemical Characterization of the Mutant Protein and Nucleotide Affinity.** Recombinant H-Ras (A18T) protein was prepared from *Escherichia coli* using the ptac expression system as described (23). The nucleotide-free form of this mutant was prepared as described for H-Ras (24). The fluorescent derivatives of GDP (guanosine 5′-diphosphate) and GppNHp (a nonhydrolyzable GTP analogue), mGDP, and mGppNHp were synthesized as described (24). Ras(A18T)·mGDP and Ras(A18T)·mGppNHp were prepared by loading nucleotide-free Ras proteins with a 1.5-fold molar excess of the fluorescent nucleotide. Excess nucleotide was separated from nucleotide-bound Ras by gel filtration on prepacked NAP-5 columns (Pharmacia, Uppsala, Sweden). Nucleotide-bound Ras(A18T) concentration was determined by high-performance liquid chromatography on a $C_{18}$ reversed phase column (Bishoff, Leonberg) as described (23). All fluorescence measurements were performed using an excitation wavelength of 366 nm and an emission wavelength of 450 nm in 30 mM Tris/HCl (pH 7.5), 10 mM $MgCl_2$, 3 mM dithioerythritol at 25°C. The nucleotide dissociation kinetics of 0.1 μM mGDP- and mGppNHp-bound Ras(A18T) in the presence of 50 μM nonlabeled GDP/GppNHp were performed on an LS50B Perkin-Elmer spectrofluorometer as described (25). The fitted curve was obtained using a single exponential equation using the program Grafit (Erithacus software).

The nucleotide association kinetics were measured by mixing 1 μM nucle-

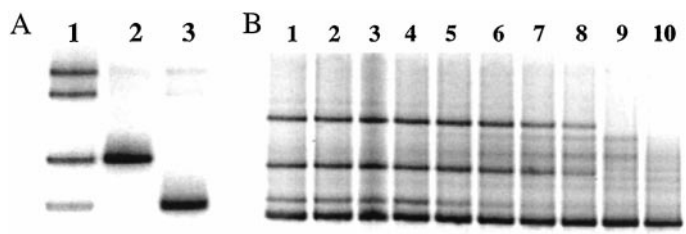


Fig. 1. Sensitivity of the DGGE mutation detection assay. *A*, to demonstrate the sensitivity of the DGGE, a mutant sample (*Lane 2*, codon 18 mutation) was mixed with a wild-type sample (*Lane 3*) to generate heteroduplexes (*Lane 1*). Mutations were clearly resolved by showing a band pattern deviant from that of the wild type. *B*, DNA from the MOLT-4 cell line (heterozygous for mutation in N-*ras* codon 12 position 1) was serially diluted with normal human spleen and revealed a detection sensitivity of 2.5% mutant DNA in wild-type DNA. *Lanes 1–9* represent the dilution of the MOLT-4 cell line (100, 80, 60, 40, 20, 10, 5, 2.5, and 0% in *Lane 9*). *Lane 10*, a wild-type pattern of a wild-type sample.

Table 1 *Results of DGGE mutation screening*

| Diagnosis | *n* | Wild type | Cod. 12[a] mut | Cod. 18[a] mut | Cod. 61[a] mut |
|---|---|---|---|---|---|
| Common acq. nevi[b] | 6 | 5 | 1 | | |
| Congenital nevi | 1 | | 1 | | 1 |
| Dysplastic nevi | 2 | | 1 | 1 | 1 |
| Clark I and LM | 2 | | 1 | 1 | |
| Clark II | 7 | 6 | | 1 | |
| Clark III | 15 | 8 | 3 | 3 | 2 |
| Clark IV | 37 | 24 | 9 | 5 | 7 |
| Clark V | 8 | 7 | 1 | | |
| Metastases | 21 | 23 | 6 | | 8 |
| Total | 111 | 73 (66%) | 23 (21%) | 11 (10%) | 19 (17%) |

[a] Mutations (mut) are seen in codon (Cod.) 12 and 18 of N-*ras* exon 1 and in codon 61 of N-*ras* exon 2.

[b] Common acquired (acq) nevi: 1 dermal nevus; 1 lentigo benigna; 4 compound nevi.

otide free form of Ras(A18T) with increasing amounts of mGDP and mGppNHp on a Applied Photophysics SX16 MV stopped-flow apparatus as described (25). The observed rate constants were obtained from single (mGDP) and double (for mGppNHp) exponential curves fitted to data. According to a two-step binding model, a hyperbolic curve was fitted to the observed rate constants plotted against the nucleotide concentration.

**Statistical Analysis.** Baseline characteristics were compared using Fisher's exact test or the Mann Whitney test, when appropriate. Quantitative data were expressed as mean ± SD. The end point of the retrospective study was the occurrence of metastasis. Patients without evidence of metastasis were censored at the date of the most recent control or the date of death attributable to a cause unrelated to MM. The Kaplan-Meier method was used to reflect actual metastasis occurrence (26). Distributions of the occurrence of metastasis were compared for each baseline characteristic with the log-rank test (27). For all tests, significance was accepted when $P < 0.05$. Statistical analysis was performed using Statview 5.0.1 (SAS Institute) on a Power Macintosh.

## RESULTS

One hundred and two malignant lesions (69 primary MMs and 33 metastases) and 9 ncn were studied for mutations in exons 1 and 2 of the N-*ras* gene using the PCR/DGGE approach. Thirty-four (31%) samples showed bandshifts for N-*ras* exon 1 (Table 1). Of these, 13 primary MMs and 6 metastases revealed a codon 12 mutation; no codon 13 mutation was seen. Two primary MMs were associated with a benign nevus, *i.e.*, a congenital compound ncn and a dysplastic ncn; in both cases, the nevus and the primary MM carried the same codon 12 mutation. Unexpectedly, 10 primary MM showed a hitherto undescribed codon 18 mutation in N-*ras* exon 1 (Table 1; Fig. 2) in which GCA (alanine) was mutated to ACA (threonine). This codon 18 mutation was not found in any of the metastatic MM examined. Bandshifts for N-*ras* exon 2 were found in 9 (13%) primary MMs, 8 (24%) metastatic MMs, and in 2 nevi, both associated with primary MMs that also exhibited N-*ras* exon 2 mutations.

To confirm our results and to exclude the occurrence of false-positive and -negative results attributable to formalin fixation or attributable to too small amounts of DNA, 10 cases were studied in both frozen and paraffin-embedded material, and in these 10 cases, DNA was extracted both from microdissected cells as well as from whole tissue slides. These four different approaches revealed identical results on DGGE scanning.

To determine the onset of the codon 18 mutation during tumor progression, all cases with this mutation were studied by microdissection of distinctive tumor progression stages, followed by DOP-PCR (Table 2). In 9 cases, two growth phases could be discerned and used for microdissection; in the case of lentigo maligna, only the RGP was studied. As shown in Table 2, the GCA→ACA mutation in codon 18 was already present in the RGP and preserved throughout the successive growth phases but did not occur *de novo* in the invasive RGP or VGP. One case showed a dysplastic nevus in continuity with a primary MM, and the codon 18 mutation was found in both the DNA, isolated from the dysplastic nevus, as well as in the DNA isolated from the tumor cells in the RGP and VGP of the adjacent MMs. The latter case, as well as a superficial spreading MM (case 1), revealed an additional mutation in codon 61 of N-*ras* exon 2.

To exclude the possibility of polymorphism at codon 18 of N-*ras*, other paraffin-embedded tissues from 3 patients harboring a codon 18 mutation in their MMs were analyzed and revealed wild-type sequences for N-*ras*. The histopathological baseline characteristics of the primary MMs and the correlation between codon 18 mutation status and the other baseline characteristics are shown in Table 3. The primary MMs harboring a codon 18 mutation were significantly thinner than those with a mutation in codon 12 or 61. There were no other significant correlations between codon 18 mutation status and the other baseline characteristics. There were no significant correlations between the codon 12 or codon 61 mutation status and any of the other baseline characteristics.

During the mean follow-up of 40 ± 34 months, 23 of the 51 patients (45%) developed metastasis of the primary MMs after a mean time of 23 ± 7 months. The diagnosis of melanoma metastasis was based on histopathological examination of the surgically resected metastasis. Of the 23 patients who developed metastasis, 13 died after a mean survival of 20 ± 17 months, and 10 were still alive at the time of this study and have been followed for a mean of 14 ± 6 months. Of the 28 patients who did not develop metastasis, 2 patients died of a cause unrelated to MM (non-Hodgkin's lymphoma and pneumonia). The cumulative probability of developing metastasis was significantly higher for patients whose primary MMs were thicker, had no mutation of codon 18, or showed vascular invasion (Table 4; Fig. 3).

After exclusion of the 16 patients who had a mutation in codons 12 and/or 61 of N-*ras*, the study population was reduced to 35 melanoma patients, of whom 8 (23%) had a mutation in codon 18, and all of the other were free of mutations. The mean follow-up of this group was 44 ± 34 months, and 15 of these 35 patients (43%) developed metastatic disease after a mean time of 23 ± 16 months. There was no significant correlation between codon 18 mutation status on the one hand and the other baseline characteristics. The cumulative probability of developing metastasis for this group was also significantly higher for male patients and for patients whose primary MMs were thicker, had no mutation of codon 18, or showed vascular invasion ($P = 0.0159$; $P = 0.0027$; $P < 0.0227$; $P < 0.0001$ respectively; data not shown).

To study the biochemical consequences of the GCA→ACA codon 18 mutation, H-Ras(A18T) was expressed in *Escherichia coli*, and the mutant protein was isolated at high purity. Although less stable than wild type, we were able to isolate this mutant protein in a nucleotide-free form, which was then used to determine the nucleotide binding properties. Dissociation and association rate constants were 2- and

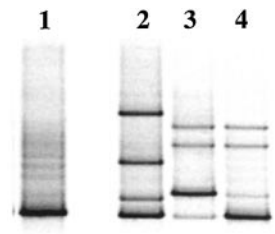


Fig. 2. Identification of mutations in exon 1 of the N-*ras* gene by DGGE analysis. DGGE band patterns of a wild-type control sample (*Lane 1*), MOLT-4 cell line (heterozygous for mutation in N-*ras* codon 12 position 1, *Lane 2*) and two unknown samples (*Lanes 3* and *4*). Both unknown samples carry the codon 18 mutation (alanine to threonine) in N-*ras* exon 1.

Table 2 *Histological and clinical features of N-RAS mutated pigment cell lesions*

| No. | Sex | Histology[a] | Anatomical site | Mutations | | Thickness (mm) | Prognostic variables[c] | | | | | Follow-up | Outcome[d] |
|---|---|---|---|---|---|---|---|---|---|---|---|---|---|
| | | | | COD 18[b] | 12/61 | | MI | ULC | REGR | TIL | INV | | |
| 1 | F | SSMM III | Buttock | RGP | 61[e] | 0.65 | <0.1 | − | − | NB | − | 26 mo | DOD |
| | | | | VGP | 61[e] | | | | | | | | |
| 2 | F | SSMM IV | Leg | RGP | | 2.82 | >6 | + | + | NB | − | 146 mo | NED |
| | | | | VGP | | | | | | | | | |
| 3 | F | SSMM III | Knee | RGP | | 2.40 | <0.1 | − | + | NB | − | 109 mo | NED |
| | | | | VGP | | | | | | | | | |
| 4 | M | SSMM II | Leg | RGP | | 0.50 | <0.1 | − | − | B | − | 44 mo | NED |
| | | | | iRGP | | | | | | | | | |
| 5 | F | SSMM III | Leg | RGP | | 0.85 | <0.1 | − | + | − | − | 49 mo | NED |
| | | | | VGP | | | | | | | | | |
| 6 | M | DYSPL.NCN | Upper arm | DYSPL.NCN | 61[f] | | | | | | | | |
| | | SSMM IV | | RGP | 61[f] | 1.60 | >6 | + | + | NB | − | 25 mo | NED[g] |
| | | | | VGP | 61[f] | | | | | | | | |
| 7 | F | SSMM IV | Thigh | RGP | | 1.38 | 0.1–6 | + | + | − | − | 42 mo | NED |
| | | | | iRGP | | | | | | | | | |
| 8 | M | LM | Forehead | RGP | | | | − | − | − | − | 16 mo | NED |
| 9 | F | SSMM IV | Arm | RGP | | 1.7 | 0.1–6 | + | − | NB | + | 76 mo | NED |
| | | | | VGP | | | | | | | | | |
| 10 | M | ALMM IV | Foot | RGP | | 2.2 | 0.1–6 | − | + | NB | − | 91 mo | NED[g] |
| | | | | VGP | | | | | | | | | |
| 11 | F | ALMM V | Foot | | | 4.27 | >6 | − | − | − | − | 14 mo | DOD |
| | | +M | | | 61[f] | | | | | | | | |
| 12 | F | NMM IV | Upper arm | | 61[f] | 2.30 | >6 | + | − | NB | − | 19 mo | DOD |
| | | +M | | | 61[f] | | | | | | | | |
| 13 | M | ALMM IV | Foot | | | 2.40 | 0.1–6 | + | − | − | + | 11 mo | DOD |
| | | +M | | | 61[f] | | | | | | | | |
| 14 | F | NMM IV | Back | | 12[h] | 3.39 | >6 | + | − | − | − | 41 mo | DOD |
| | | +M | | | 12[h]/61[e] | | | | | | | | |
| 15 | M | SSMM IV | Back | | 12[h]/61[e] | 1.4 | <0.1 | + | + | B | − | 34 mo | DOD |
| | | +M | | | 12[h]/61[e] | | | | | | | | |
| 16 | F | ALMM IV | Foot | | 12[h] | 3.79 | 0.1–6 | + | + | − | − | 28 mo | SMD |
| | | +M | | | 12[h] | | | | | | | | |
| 17 | M | SSMM III | Upper arm | | 12[h] | 2.78 | <0.1 | − | − | − | − | 14 mo | SMD |
| | | +M | | | 12[h] | | | | | | | | |
| 18 | F | ALMM IV | Foot | | 12[h] | 2.62 | 0.1–6 | + | + | − | + | 19 mo | in tr.M NED |
| 19 | F | M[i] | Leg | | 61[j] | | | | | | | 44 mo | NED |
| 20 | F | SSMM IV | Back | | 12[h]/61[k] | 1.95 | >6 | − | + | − | − | 1 mo | NED |
| 21 | M | SSMM IV | Back | | 12[h]/61[k] | 2.78 | >6 | + | − | − | − | 41 mo | NED |
| 22 | M | SSMM IV | Leg | | 12[h] | 2.7 | 0.1–6 | ++ | + | − | + | 5 mo | NED |
| | | +M | | | 12[h] | | | | | | | | |
| 23 | F | ALMM IV | Foot | | 12[h]/61[f] | 2.2 | 0.1–6 | − | − | B | − | 107 mo | NED |

[a] SSMM, superficial spreading MM; ALMM, acral lentiginous MM; NMM, nodular MM; M, metastasis.
[b] All growth phases of the first 8 cases and none of the other cases carried the codon 18 mutation (GCA→ACA).
[c] MI, mitotic index (mitoses/mm$^2$); ULC, ulceration; REGR, regression; B, brisk; NB, non-brisk; −, absent; INV, invasion of blood or lymph vessels.
[d] DOD, dead of disease; NED, no evidence of disease; SMD, stable metastatic disease; in tr.M, in transit M.
[e] Codon 61 mutation (CAA→AAA).
[f] Codon 61 mutation (CAA→CGA).
[g] Patient died of a non-melanoma related cause.
[h] Codon 12 mutations were in all cases a transition from GGT (glycine) to GAT (asparagine).
[i] Primary MM could not be evaluated.
[j] Codon 61 mutation (CAA→CTA).
[k] Codon 61: sequencing failed, unknown base change.

4-fold faster, resulting in GDP/GppNHp affinities that were remarkably similar to those measured for Ras wild type (Fig. 4; Table 5; Ref. 25).

## DISCUSSION

Several techniques have been used to analyze *ras* gene mutations in human tumors. NIH 3T3 transfection assays using either *in vitro* or *in vivo* selection are laborious and time consuming and may introduce selection artifacts (28, 29). Hybridization techniques would miss any exon 1 and 2 mutations other than those targeted by the specific probes chosen for the assay and are often not sensitive enough to distinguish between wild-type and mutated alleles (9, 19, 30). RFLP assays are normally limited to the detection, in each setting, of a base change at only two positions in one codon of a *ras* gene or even to the detection of only one specific *ras* mutation (31, 32). SSCP and DGGE are now the two major techniques in mutation scanning. SSCP is less sensitive than DGGE and is more dependent on the length of the fragment (33). Sensitivity of mutation detection by SSCP falls dramatically with increasing length of the analyzed fragment. To overcome these problems, we have chosen for the DGGE technique to study mutations in N-*ras* exons 1 and 2 in a large series of MMs. To the best of our knowledge, this is the first time that DGGE scanning is used to detect N-*ras* gene mutations in MM.

Analyzing N-*ras* mutations in a large group of MM, we could distinguish three groups of patients, *i.e.*, a group without mutations, a group with the classical activating point mutations in codons 12 and 61, and a group of patients with a novel point mutation in codon 18 of N-*ras* exon 1. The latter mutation occurred in 10 of 102 (10%) malignant pigment cell lesions and resulted in a substitution of alanine (GCA) by threonine (ACA). This mutation was found in tumor DNA derived from both frozen and formalin-fixed tissue section, and the same results were obtained when DNA was extracted from whole tissue sections (immediately used for specific PCR), as well as when DNA was obtained from small numbers of cells (microdissected from distinctive stages of tumor progression in frozen or paraffin-embed-

Table 3 *Clinical and histopathological baseline characteristics and their correlation with codon 18 mutation status*

| Baseline characteristic | All patients *n* (%)[a] | Patients without codon 18 mutation *n* (%)[a] | Patients with codon 18 mutation *n* (%)[a] | *P*[b] |
|---|---|---|---|---|
| | 51 | 41 | 10 | |
| Age | 67 ± 19 | 68 ± 19 | 66 ± 20 | |
| Sex | | | | 0.8125 |
| Male | 24 (47) | 20 (49) | 4 (40) | |
| Female | 27 (53) | 21 (51) | 6 (60) | |
| Breslow | 2.85 ± 3.30 | 3.21 ± 3.65 | 1.37 ± 0.88 | 0.0257 |
| ≤2 mm | 23 (45) | 15 (36) | 8 (80) | 0.0298 |
| >2 mm | 28 (55) | 26 (64) | 2 (20) | |
| Mitotic index | | | | 0.9999 |
| ≤6/mm$^2$ | 41 (80) | 33 (80) | 8 (80) | |
| ≥6/mm$^2$ | 10 (20) | 8 (20) | 2 (20) | |
| TIL | | | | 0.4949 |
| Absent | 30 (59) | 23 (56) | 7 (70) | |
| Present | 21 (41) | 18 (44) | 3 (30) | |
| Ulceration | | | | 0.4853 |
| Absent | 24 (47) | 18 (44) | 6 (60) | |
| Present | 27 (53) | 23 (66) | 4 (40) | |
| Regression | | | | 0.2952 |
| Absent | 29 (57) | 25 (61) | 4 (40) | |
| Present | 22 (43) | 16 (39) | 6 (60) | |
| Vascular invasion | | | | 0.4190 |
| Absent | 38 (75) | 29 (71) | 9 (90) | |
| Present | 13 (25) | 12 (29) | 1 (10) | |
| Codon 12 mutation | | | | 0.0920 |
| Absent | 39 (77) | 29 (71) | 10 (100) | |
| Present | 12 (23) | 12 (29) | 0 (0) | |
| Codon 61 mutation | | | | 0.2499 |
| Absent | 46 (90) | 38 (93) | 8 (80) | |
| Present | 5 (10) | 3 (7) | 2 (20) | |

[a] Values in parentheses are column percentages.
[b] Fisher's exact test or Mann-Whitney test.

ded sections), amplified by DOP-PCR and followed by specific PCR. Because these different approaches gave the same results, the observed novel point mutation is very unlikely to be artificially induced by preparation of the specimen or by the PCR procedure itself (34). Other nonmelanoma tissues from 3 patients harboring the codon 18 mutation in their MMs were analyzed by the same method but revealed only wild-type N-*ras*, thus excluding the possibility of polymorphism. Therefore, our data indicate that a novel mutation in codon 18 of the first exon of N-*ras* involving a GCA→ACA transition should be added to the range of point mutations already known to occur in this oncogene. Whether this mutation is specific for MM will require extensive analysis of other cancers with the same method; our preliminary results in a series of colonic and pancreatic adenocarcinomas and neuroblastomas have not revealed a similar N-*ras* codon 18 mutation.[4] Our study also illustrates the high sensitivity of the DGGE technique, which recently allowed the detection of a new mutation in another gene in MM (35).

Analyzing distinctive stages of tumor progression in MM by microdissection, the codon 18 GCA→ACA mutation was found to occur already in the "pure" RGP and to be preserved throughout the successive growth phases of the primary MM; in none of the cases was this mutation found to arise *de novo* in the invasive RGP or VGP. Previous studies have claimed that mutations in N-*ras* are restricted to the VGP (14). Using microdissection, we have shown that activating mutations in codon 61 of N-*ras* are already present in the RGP (*i.e.*, cases 1 and 6; Table 2), and these mutations remain preserved during subsequent tumor progression phases, thus confirming a recent study that N-*ras* mutations contribute to MM progression from the RGP to the VGP (36).

One MM with an adjacent dysplastic nevus revealed identical codon 18 (GCA→ACA) and codon 61 (CAA→CGA) mutations in both components of the pigment cell lesion. Although it is generally accepted that dysplastic nevi are markers to identify patients who are at increased risk to develop MM, there is much debate as to whether these dysplastic nevi actually serve as precursors of MM. Our demonstration of identical N-*ras* mutations at two different codons of N-*ras* in the DNA of both the dysplastic nevus as well as the adjacent MM strongly suggests a clonal relationship between both lesions.

The clinical follow-up of the patients with codon 18 mutation indicates an excellent prognosis as compared with patients with a MM harboring classical activating point mutations in codons 12 or 61 or

Table 4 *Clinical and histopathological baseline characteristics in relation to the occurrence of metastasis*

| | *n* 51 | Patients with metastasis n (%)[a] 23 (45) | *P*[b] |
|---|---|---|---|
| Codon 18 mutation | | | |
| Absent | 41 | 22 (54) | 0.0130 |
| Present | 10 | 1 (10) | |
| Codon 12 mutation | | | |
| Absent | 39 | 17 (44) | 0.4921 |
| Present | 12 | 6 (50) | |
| Codon 61 mutation | | | |
| Absent | 46 | 20 (43) | 0.5571 |
| Present | 5 | 3 (60) | |
| Breslow | | | 0.0115 |
| <1.0 mm | 10 | 2 (20) | |
| 1.01–2.0 mm | 12 | 3 (25) | |
| 2.01–4.0 mm | 22 | 13 (52) | |
| >4.0 mm | 7 | 5 (71) | |
| Age | | | 0.7783 |
| ≤55 years | 12 | 5 (42) | |
| >55 years | 39 | 19 (49) | |
| Sex | | | 0.0568 |
| Male | 24 | 14 (59) | |
| Female | 27 | 9 (33) | |
| Mitotic index | | | 0.4785 |
| ≤6/mm$^2$ | 41 | 18 (44) | |
| >6/mm$^2$ | 10 | 5 (50) | |
| TIL | | | 0.2773 |
| Absent | 30 | 12 (40) | |
| Present | 21 | 11 (52) | |
| Ulceration | | | 0.1881 |
| Absent | 24 | 8 (33) | |
| Present | 27 | 15 (55) | |
| Regression | | | 0.2528 |
| Absent | 29 | 15 (52) | |
| Present | 22 | 8 (36) | |
| Vascular invasion | | | 0.0006 |
| Absent | 38 | 13 (34) | |
| Present | 13 | 10 (77) | |

[a] Values in parentheses are row percentages.
[b] Log-rank test.

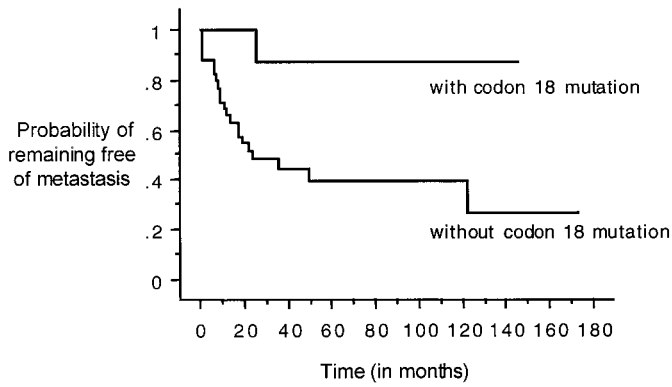


Fig. 3. Cumulative probability of remaining free of metastasis for patients with and without codon 18 mutation. Statistical analysis was done on a group of 51 patients that had been followed for at least 6 months after resection of the tumor. The end point of the retrospective study was the occurrence of metastasis. The Kaplan-Meier method was used as described in "Materials and Methods." The cumulative probability of developing metastasis was significantly lower for the group of patients with a codon 18 mutation in their MMs ($P = 0.0130$).

[4] A. Demunter, C. De Wolf-Peeters, J. J. van den Cord, unpublished observations.

with wild-type MM samples. The only patient with an N-*ras* codon 18 mutation that died of melanoma also carried an activating point mutation in codon 61. This excellent prognosis is likely to be attributable to the fact that MM with N-*ras* codon 18 mutations were significantly thinner than MM carrying activating mutations at codons 12 and 61. The fact that codon 18 mutation status correlated only with the thickness of the primary MM and not with the other clinical and histopathological characteristics strongly suggest that there exists a causal relation between both parameters. In addition, when the group of codon 18 patients was compared with the group of patients with the classical mutations as well as with those without mutations, a highly significant difference in overall outcome was found, suggesting that patients with this novel mutation are favored over those without genetic aberrations in the N-*ras* gene.

Our clinical and histological data therefore suggest that this novel GCA→ACA mutation in codon 18 of N-*ras* exon 1 interferes with the Ras-dependent mitogenic signaling pathway, resulting in slower growth and hence, earlier detection. As such, screening of MM patients for mutations in codon 18 of N-*ras* exon 1 may identify a subgroup of patients with a better prognosis. Future studies on prospectively followed patients are currently under way.

The precise effect of this novel N-*ras* codon 18 mutation on the proliferation of melanoma cells in the earliest stages of tumor progression requires extensive functional assays. However, we can make some speculations, based on the biochemical properties of the Ras protein. Alanine 18 is placed at the COOH-terminal end of the highly conserved phosphate-binding motif (GXXXGKS/TA). Amino acid substitutions within this region often impair the nucleotide binding (serine 17 mutation) and GTPase reaction (glycine 12/13 mutations). More than 30% of human tumors contain a Ras protein with point mutations mainly at codons 12 and 61, more rarely at codon 13 (2).

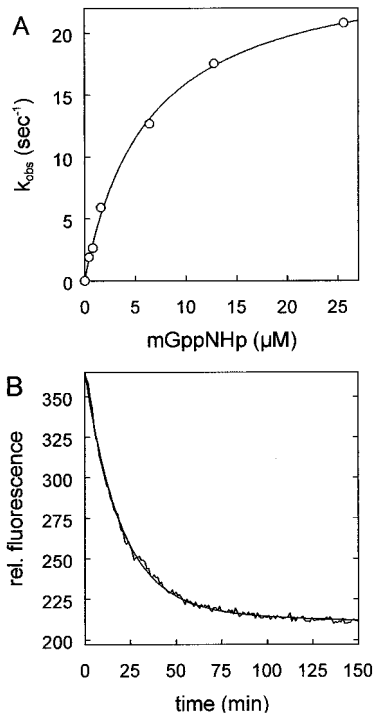


Fig. 4. Kinetics of nucleotide association (*A*) and nucleotide dissociation (*B*) with Ras(A18T). *A*, pseudo first-order rates for the interaction between Ras(A18T) and increasing concentrations of mGppNHp were determined as described in "Materials and Methods." The measured rate constants were plotted against nucleotide concentration, and the *solid line* shows the fitted hyperbolic curve. *B*, the dissociation rate constant is determined by displacement of bound mGppNHp by the 500-fold molar excess of nonlabeled GppNHp by monitoring a decrease of fluorescence with time. The curve is fitted to a single exponential.

Table 5 *Nucleotide binding of Ras wild-type and Ras(A18T) mutants*

The kinetics of two-step binding reaction were measured using fluorescent nucleotides (mGDP and mGPPNHp) as described in "Materials and Methods."

| Protein and nucleotide | $k_{on}$ ($10^6$ M$^{-1}$ s$^{-1}$) | $k_{off}$ ($10^{-5}$ s$^{-1}$) | $K_D$[a] ($10^{-10}$ M) |
|---|---|---|---|
| Ras wt[b] | | | |
| mGDP | 1.5 | 2 | 13 |
| mGppNHp | 1.8 | 36 | 200 |
| Ras(A18T) | | | |
| mGDP | 3.4 | 8.4 | 24.7 |
| mGppNHp | 4.0 | 78.3 | 195 |

[a] Calculated from the rates of dissociation and association rate constants ($K_D = k_{off}/k_{on}$).
[b] As described by Schmidt *et al.* (25).

Ras proteins with these somatic mutations have a defective GTPase activity and can no longer be switched off by GAPs. The reason behind these dramatic functional changes by codon 12 and 13 mutation of *ras* are rearrangements around the active site, resulting in displacement of catalytic amino acids such as glutamine 61 of Ras and the arginine finger of RasGAP (37, 38). Unlike these oncogenic mutants, replacement of serine 17 by an asparagine dramatically affects the nucleotide binding. This mutant binds with high affinity to the Ras-specific GEFs and thereby blocks the GEF activity in cells (39, 40).

Preliminary functional studies, aimed to detect similar nucleotide binding alterations as described for mutations in codon 17, were performed. They showed a faster dissociation rate of the codon 18 mutant Ras protein from the guanine nucleotide binding site as compared with the wild-type Ras protein. However, because of faster association, the overall affinity is only marginally affected. It is interesting to note that the homologous residue in many other GTP binding proteins is threonine or serine/cysteine (41). In the structures known, polar interactions of the side chain hydroxyl groups with α-phosphate oxygen atoms were observed (*e.g.*, EF-Tu, Ran, and others), suggesting stabilization of binding. In Ras, the structure would seemingly allow similar interactions in Ras(A18T). The GDP dissociation of N-Ras ($1.0 \times 10^5$ s$^{-1}$) is similar to that of H-Ras (Table 5; Ref. 42). Because N-Ras and H-Ras are very similar (85% identity), differing mainly in regions not involved in nucleotide interaction, we assume that the biochemical data obtained for H-Ras(A18T) can be assigned for N-Ras(A18T) mutants. Thus, in view of these preliminary findings, additional studies aimed to measure the affinity to GEFs and GAPs are needed to elucidate the role of the N-Ras(A18T) mutant in MM.

In summary, using the very sensitive DGGE approach, we have detected a novel mutation in codon 18 of N-*ras* exon 1 in 15% of the primary MMs. This mutation occurs already in the earliest stages of the tumor and seems to identify a group of melanoma patients with better prognosis than those with wild-type sequence or the classical activating point mutations in codons 12 and 61. Multivariate analysis on larger groups of patients in a prospective study should, however, be performed to elucidate the prognostic value of this codon 18 mutation.

## ACKNOWLEDGMENTS

We thank Miet Vanherck and Monique Pattou for assistance in the molecular pathology lab. We also thank Dorothee Kühlmann for preparing Ras(A18T) mutant.

## REFERENCES

1. Shih, T. Y., Weeks, M. O., Young, H. A., and Scolnick, E. M. p21 of Kirsten murine sarcoma virus is thermolabile in a viral mutant temperature sensitive for the maintenance of transformation. J. Virol., *31:* 546–546, 1979.

2. Bos, J. L. *Ras* oncogenes in human cancer: a review. Cancer Res., *49:* 4682–4689, 1989.
3. Barbacid, M. *RAS* genes. Annu. Rev. Biochem., *56:* 779–827, 1987.
4. Temeless, G. L., Gibbs, J. B., D'Alonzo, J. S., Signal, I. S., and Scolnick, E. M. Yeast and mammalian RAS proteins have conserved biochemical properties. Nature (Lond.), *313:* 700–703, 1985.
5. Sweet, R. W., Yokoyama, S., Kamata, T., Feramisco, J. R., Rosenberg, M., and Gross, M. The product of RAS is a GTPase and the T24 oncogenic mutant is deficient in this activity. Nature (Lond.), *311:* 273–275, 700–703, 1984.
6. Der, C. J., Finkel, T., and Cooper, G. M. Biological and biochemical properties of human *RASH* genes mutated at codon 61. Cell, *44:* 167–176, 1986.
7. Bar-Eli, M., Ahuja, H., Foti, A., and Cline, M. J. N-RAS mutations in T-cell acute lymphocytic leukemia: analysis by direct sequencing detects a novel mutation. Br. J. Haematol., *72:* 36–39, 1989.
8. Reddy, E. P., Reynolds, R. K., Santos, E., and Barbacid, M. A point mutation is responsible for the acquisition of transforming properties by the T24 human bladder carcinoma oncogene. Nature (Lond.), *300:* 149–152, 1982.
9. Bos, J. L., Toksoz, D., Marshall, C. J., Verlaan-de Vries, M., Veeneman, G. H., van der Eb, A. J., van Boom, J. H., Janssen, J. W., and Steenvoorden, A. C. Amino-acid substitutions at codon 13 of the N-*RAS* oncogene in human acute myeloid leukemia. Nature (Lond.), *315:* 726–730, 1985.
10. Dhar, R., Ellis, R. W., Shih, T. Y., Oroszlan, S., Shapiro, B., Maizel, J., Lowy, D., and Scolnick, E. Nucleotide sequence of the p21 transforming protein of Harvey murine sarcoma virus. Science (Wash. DC), *217:* 934–936, 1982.
11. Taparowsky, E., Shimuzu, K., Goldfarb, M., and Wigler, M. Structure and activation of the human N-*RAS* gene. Cell, *34:* 581–586, 1983.
12. Albino, A. P., Nanus, D. M., and Mentle, I. R., Cordon-Cardo, C., McNutt, N. S., Bressler, J., and Andreeff, M. Analysis of *RAS* oncogenes in malignant melanoma and precursor lesions: correlation of point mutations with different phenotype. Oncogene, *4:* 1363–1374, 1989.
13. van't Veer, L. J., Burgering, B. M. T., Versteeg, R., Boot, A. J. M., Ruiter, D. J., Osanto, S., Schrier, P. I., and Bos, J. L. N-*RAS* mutations in human cutaneous melanoma from sun-exposed body sites. Mol. Cell. Biol., *9:* 3114–3116, 1989.
14. Ball, N. J., Yohn, J. J., Morelli, J. G., Norris, D. A., Golitz, L. E., and Hoeffler, J. P. RAS mutations in human melanoma: a marker of malignant progression. J. Investig. Dermatol., *102:* 285–290, 1994.
15. Van der Lubbe, J. L. M., Rosdorff, H. J. M., Bos, J. L., and Van der Eb, A. J. Activation of N-RAS induced by ultraviolet irradiation *in vitro*. Oncogene Res., *3:* 9–20, 1988.
16. Schrier, P. I., Versteeg, R., Peltenburg, L. T., Plomp, A. C., van't Veer, L. J., and Kruse-Wolters, K. M. Sensitivity of melanoma cell lines to natural killer cells: a role for oncogene-modulated HLA class I expression? Semin. Cancer Biol., *2:* 73–83, 1991.
17. Verlaan de Vries, M., Bogaard, M. E., Van den Elst, H., Van Boom, J. H., Van der Eb, A. J., and Bos, J. L. A dot-blot screening procedure for mutated *RAS* oncogenes using synthetic oligonucleotides. Gene (Amst.), *50:* 313–320, 1986.
18. Balch, C. M., Buzaid, A. C., Atkins, M. B., Cascinelli, N., Coit, D. G., Fleming, I. D., Houghton, A., Kirkwood, J. M., Mihm, M. F., Morton, D. L., Reintgen, D., Ross, M. I., Sober, A., Soong, S. J., Thompson, J. A., Thompson, J. F., Gershenwald, J. E., and McMasters, K. M. A new American Joint Committee on Cancer staging system for cutaneous melanoma. Cancer (Phila.), *88:* 1484–1491, 2000.
19. Elder, D. E., and Murphy, G. F. Melanocytic tumors of the skin. *In:* J. Rosai and L. H. Sobin (eds.), Atlas of Tumor Pathology, pp. 154–161. Washington DC: Armed Forces Institute of Pathology, 1990.
20. Telenius, H., Nigel, P. C., Bebb, C. E., Nordenskjold, M., Ponder, B. A. J., and Tunnacliffe, A. Degenerate oligonucleotide-primed PCR: general amplification of target DNA by a single degenerate primer. Genomics, *13:* 718–725, 1992.
21. Kuukasjarvi, T., Tanner, M., Pennanen, S., Karhu, R., Visakorpi, T., and Isola, J. Optimizing DOP-PCR for universal amplification of small DNA samples in comparative genomic hybridization. Genes Chromosomes Cancer, *18:* 94–101, 1997.
22. Neri, A., Knowles, D. M., Greco, A., and McCormick, F. Analysis of *RAS* oncogene mutations in human lymphoid malignancies. Proc. Natl. Acad. Sci. USA, *85:* 9268–9272, 1988.
23. Tucker, J., Sczakiel, G., Feuerstein, J., John, J., Goody, R. S., and Wittinghofer, A. Expression of p21 proteins in *Escherichia coli* and stereochemistry of the nucleotide-binding site. EMBO J., *5:* 1351–1358, 1986.
24. John, J., Sohmen, R., Feuerstein, J., Linke, R., Wittinghofer, A., and Goody, R. S. Kinetics of interaction of nucleotides with nucleotide-free H-ras p21. Biochemistry, *29:* 6058–6065, 1990.
25. Schmidt, G., Lenzen, C., Simon, I., Deuter, R., Cool, R. H., Goody, R. S., and Wittinghofer, A. Biochemical and biological consequences of changing the specificity of p21ras from guanosine to xanthosine nucleotides. Oncogene, *12:* 87–96, 1996.
26. Kaplan, E. L., and Meier, P. Nonparametric estimation from incomplete observations. J. Am. Stat. Assoc., *53:* 457–481, 1958.
27. Peto, R., and Peto, J. Asymptomatically efficient rank invariant procedures. J. R. Stat. Soc. A, *135:* 185–207, 1972.
28. Eva, A., Tronick, S. R., Col, R. A., Pierce, J. H., and Aaronson, S. A. Transforming genes of human hematopoietic tumors. Frequent detection of *RAS*-related oncogenes whose activation appears to be independent of tumor phenotype. Proc. Natl. Acad. Sci. USA, *80:* 4926–4930, 1983.
29. Hirai, H., Tanaka, S., Azuma, N., Anraku, Y., Kobayashi, Y., Fujisaria, M., Okabe, T., Urabe, A., and Takaku, F. Transforming genes in human leukemia cells. Blood, *66:* 1371–1378, 1985.
30. Farr, C. J., Saiki, R. K., Erlich, H. A., McCormick, P., and Marshall, C. J. Analysis of *RAS* gene mutations in acute myeloid leukemia by polymerase chain reaction and oligonucleotide probes. Proc. Natl. Acad. Sci. USA, *85:* 1629–1633, 1988.
31. Jiang, W., Kahn, S. M., Guillem, J. G., Lu, S. H., and Weinstein, I. B. Rapid detection of *RAS* oncogenes in human tumors: applications to colon, esophageal, and gastric cancer. Oncogene, *4:* 923–928, 1989.
32. Lin, S. Y., Chen, P. H., Yang, M. J., Chen, T. C., Chang, C. P., and Chang, J. G. *RAS* oncogene and *p53* gene hotspot mutations in colorectal cancers. J. Gastroenterol. Hepatol., *10:* 119–124, 1995.
33. Condie, A., Eeles, R., Borresen, A. L., Coles, C., Cooper, C., and Prosser, J. Detection of point mutations in the *p53* gene: comparison of single-strand conformation polymorphism, constant denaturant gel electrophoresis, and hydroxylamine and osmium tetroxide techniques. Hum. Mutat., *2:* 58–66, 1993.
34. Williams, C., Pontén, F., Moberg, C., Söderkvist, P., Uhlén, M., Pontén, J., Sitbon, G., and Lundeberg, J. A high frequency of sequence alterations is due to formalin fixation of archival specimens. Am. J. Pathol., *155:* 1467–1471, 1999.
35. Guldberg, P., Kirkin, A. F., Gronbaek, K., Straten, P. T., Ahrenkiel, V., and Zeuthen, J. Complete scanning of the *CDK4* gene by denaturing gradient gel electrophoresis: a novel missense mutation but low overall frequency of mutations in sporadic metastatic malignant melanoma. Int. J. Cancer, *72:* 780–783, 1997.
36. Shellman, Y. G., Chapman, J. T., Fujita, M., Norris, D. A., and Maxwell, I. H. Expression of activated N-*ras* in a primary melanoma cell line counteracts growth inhibition by transforming growth factor-$\beta$. J. Investig. Dermatol., *114:* 1200–1204, 2000.
37. Krengel, U., Schlichting, L., Scherer, A., Schumann, R., Frech, M., John, J., Kabsch, W., Pai, E. F., and Wittinghofer, A. Three-dimensional structures of H-ras p21 mutants: molecular basis for their inability to function as signal switch molecules. Cell, *62:* 539–548, 1990.
38. Scheffzek, K., Ahmadian, M. R., Kabsch, W., Wiesmüller, L., Lautwein, A., Schmitz, F., and Wittinghofer, A. The Ras-RasGAP complex: structural basis for GTPase activation and its loss in oncogenic Ras mutants. Science (Wash. DC), *277:* 333–338, 1997.
39. Cool, R. H., Schmidt, G., Lenzen, C. U., Prinz, H., Vogt, D., and Wittinghofer, A. The Ras mutant D119N is both dominant negative and activated. Mol. Cell. Biol., *19:* 6297–6305, 1999.
40. Stacey, D. W., Feig, L. A., and Gibbs, J. B. Dominant inhibitory Ras mutants selectively inhibit the activity of either cellular or oncogenic Ras. Mol. Cell. Biol., *11:* 4053–4064, 1991.
41. Bourne, H. R., Sanders, D. A., and McCormick, F. The GTPase superfamily: conserved structure and molecular mechanism. Nature (Lond.), *349:* 117–127, 1991.
42. Lenzen, C., Cool, R. H., Prinz, H., Kuhlmann, J., and Wittinghofer, A. Kinetic analysis by fluorescence of the interaction between Ras and the catalytic domain of the guanine nucleotide exchange factor Cdc25Mm. Biochemistry, *37:* 7420–7430, 1998.

# A Novel N-*ras* Mutation in Malignant Melanoma Is Associated with Excellent Prognosis

Anouk Demunter, Mohammad Reza Ahmadian, Louis Libbrecht, et al.

*Cancer Res* 2001;61:4916-4922.